Research Square

Preprints are preliminary reports that have not undergone peer review.
They should not be considered conclusive, used to inform clinical practice,
or referenced by the media as validated information.

Effects of Rht-B1p, Ppd-D1b and Vrn-B1 on agronomic traits in a family-structured spring wheat population across multiple years and environments: an open and reproducible workflow combining mixed models and multivariate analyses

Pavel Kroupin
All-Russian Research Institute of Agricultural Biotechnology
Lubov Nazarova
All-Russian Research Institute of Agricultural Biotechnology
Vladimir Panchenko
P.P. Lukyanenko National Grain Center
Viktoria Voronezhskaya
All-Russian Research Institute of Agricultural Biotechnology
Ludmila Bespalova
P.P. Lukyanenko National Grain Center
Anastasiya Chernook
All-Russian Research Institute of Agricultural Biotechnology
Aleksandra Kroupina
All-Russian Research Institute of Agricultural Biotechnology
Gennady Karlov
All-Russian Research Institute of Agricultural Biotechnology
Mikhail Divashuk
divashuk@gmail.com

All-Russian Research Institute of Agricultural Biotechnology

Research Article

Keywords: Rht, Ppd, Vrn, Triticum aestivum L., LMM, ICC, PERMANOVA, GGE

Posted Date: September 7th, 2026

DOI: https://doi.org/10.21203/rs.3.rs-10626349/v1

License: This work is licensed under a Creative Commons Attribution 4.0 International License. Read Full License

Additional Declarations: No competing interests reported.

Abstract

Background

Bread wheat (*Triticum aestivum L.*) adaptation to contrasting environments is governed by major genes controlling plant height (*Rht*), photoperiod response (*Ppd*) and vernalisation requirement (*Vrn*). However, their pleiotropic effects and interactions are often studied in isolation, without accounting for family background or applying multivariate approaches. Here we evaluated a large spring wheat population (n = 4107 individual plant observations from 81 unique families, $F_{3:4}$-$F_{5:6}$) segregating for *Rht-B1p* (a semi-dwarf allele), *Ppd-D1b* (a photoperiod-sensitive allele) and *Vrn-B1a* (a spring habit allele) across five location–year environments during a three-year field study conducted at two locations (Krasnodar 2018, 2019; Moscow 2018, 2019, 2022). We combined univariate year-specific and pooled mixed-model analyses with multivariate approaches to evaluate gene and environment effects. Family structure was accounted for by including family as a random effect in the linear mixed models (LMM), and intraclass correlation (ICC) coefficients were estimated to quantify within-family similarity.

Results

The semi-dwarfing allele *Rht-B1p* consistently reduced plant height by 18–38 cm across environments ($P < 0.001$) and showed environment-dependent effects on calculated thousand-grain weight and grain weight per spike. *Vrn-B1* had only minor, environment-specific effects, likely owing to the fixed *Vrn-A1a* background. Mean LDA accuracy was 96.7% for *Rht-B1*, 72.3% for *Ppd-D1*, and 63.0% for *Vrn-B1*, while Mahalanobis (D^2) values were greatest for the *Rht-B1p/Rht-B1a* contrast (6.8–47.8). Family effects were substantial, with ICC values for plant height reaching 0.95, emphasising the need to account for relatedness. GGE biplot analysis identified *Rht-B1a/Ppd-D1b* as the best-performing combination for grain weight per spike in Moscow 2022, whereas *Rht-B1p/Ppd-D1b* provided the most favourable compromise between reduced stature and competitive productivity. This combination may therefore be useful when both yield and reduced lodging risk are breeding priorities, although lodging resistance was not assessed directly.

Conclusions

We conclude that the *Rht-B1p* allele was the strongest multivariate discriminator among the three loci, whereas the *Vrn-B1a* versus *vrn-B1* contrast had only minor, environment-specific effects in a *Vrn-A1a* background. Family structure must therefore be accounted for to obtain unbiased effect estimates. These results provide a robust framework for marker-assisted selection of optimal allele combinations for specific agro-ecological zones.

Background

Wheat (*Triticum aestivum L.*) is a cornerstone of global food security, supplying approximately 20% of the world's calories and protein. With growing demand and increasing pressure from climate change, breeding for high-yielding, stable, and well-adapted wheat varieties remains a top priority. The adaptability of wheat to diverse agro-ecological zones is largely governed by a few major genes controlling plant height, vernalisation requirement and photoperiod sensitivity – collectively referred to as "adaptation genes". Understanding how

these genes interact with each other and with the environment is essential for designing resilient, high-performing cultivars.

Dwarfing genes: from Green Revolution to alternative sources

The "Green Revolution" of the 1960s was driven by the introduction of semi-dwarfing alleles *Rht-B1b* and *Rht-D1b*, which reduced plant height, prevented lodging, and improved harvest index under high-input conditions [1–3]. However, these GA-insensitive alleles also have undesirable pleiotropic effects, such as reduced coleoptile length and lower thousand-grain weight [3, 4]. Alternative dwarfing sources, such as the GA-insensitive *Rht-B1p* (formerly designated *Rht17*), have been described and characterised in spring wheat [5, 6]. The *Rht-B1p* encodes a DELLA-protein and results in gibberellin-insensitive dwarfing [5]. In bread wheat, it reduces plant height by approximately 30% under greenhouse conditions [5], while in durum wheat the reduction can reach 40–48% in field experiments [7]. In our previous study of the same spring wheat population, we evaluated the pleiotropic effects of *Rht-B1p* in combination with *Vrn-B1* and *Ppd-D1* alleles under contrasting field conditions in Moscow and Krasnodar [6]. However, that experiment covered only a single growing season (2018) and therefore could not assess the temporal stability or year dependence of the observed genetic effects. The present study extends this earlier work using an expanded multi-year dataset and a family-adjusted, multi-environment analytical framework.

Photoperiod and vernalisation genes: modulators of phenology and yield

Flowering time in wheat is primarily controlled by the vernalisation genes *Vrn-1* (on chromosomes 5A, 5B and 5D) and the photoperiod response genes *Ppd-1* (on chromosomes 2A, 2B and 2D) [8, 9]. Dominant alleles at *Vrn-1* confer spring growth habit, while recessive alleles result in winter habit. The photoperiod-insensitive allele *Ppd-D1a* is widespread in low-latitude regions where early flowering helps escape heat and drought [8, 10], whereas the sensitive allele *Ppd-D1b* predominates in high-latitude environments with long summer days [11]. The strength of *Ppd-D1* effects varies with genetic background and day length; *Ppd-D1* can explain 12.1–19.0% of phenotypic variation in developmental phases [12]. Importantly, *Ppd-D1* also affects spike fertility and grain weight [13], and its interaction with dwarfing genes can modify plant height and yield components [14, 15].

The influence of *Vrn-B1* is largely masked by *Vrn-A1a*, but this does not preclude its involvement in epistatic interactions with *Ppd-D1* [16, 17]. Recent studies in Japanese wheat have further demonstrated that the effects of *Vrn-1* and *Ppd-1* alleles on heading time depend strongly on the environment [18], highlighting the need for multi-environment evaluations.

The challenge of family structure and multivariate analysis

Despite extensive research on individual genes, systematic evaluation of the *Rht-B1p*, *Ppd-D1b*, and *Vrn-B1a* alleles across multiple environments remains limited. Most previous studies focused on a single gene or a restricted set of traits, often within a single environment. In our previous study, Kroupin et al. (2020) examined *Rht-B1p* in combination with contrasting alleles at the *Vrn-B1* (*Vrn-B1a* and *vrn-B1*) and *Ppd-D1* (*Ppd-D1a* and *Ppd-D1b*) loci at two locations, Moscow and Krasnodar. However, that analysis did not account for family

background or apply multivariate methods to characterise the joint pleiotropic effects of these loci [6]. Moreover, the effect of *Ppd-D1b* on spike fertility and grain weight is still debated [13], and the role of *Vrn-B1* in modulating the phenotypic expression of dwarfing alleles remains unclear, particularly in genetic backgrounds carrying dominant *Vrn-A1a* [19, 20]. Another important but often overlooked issue is the confounding effect of genetic relatedness (family structure) in biparental populations. Many apparent gene effects may actually arise from linked background loci or from shared family ancestry. Therefore, mixed-linear models that include family as a random effect are necessary to obtain unbiased estimates of gene effects [21]. Furthermore, traditional univariate analyses fail to capture the multivariate nature of agronomic performance. Recent advances in wheat genomics emphasise the need for integrated multivariate approaches – such as principal component analysis (PCA), canonical variate analysis (CVA), linear discriminant analysis (LDA), and genotype × environment (GGE) biplots – to dissect complex trait variation [14, 22].

Aims of this study

In this study, we used a large spring bread wheat population (M17, n = 4107) segregating for *Rht-B1p*, *Ppd-D1b* and *Vrn-B1a* across five environments (Krasnodar 2018, 2019; Moscow 2018, 2019, 2022). We aimed to: (1) quantify single-gene effects and two-way interactions, accounting for family structure; (2) compare the multivariate discriminatory power of the three genes using PCA, LDA and Mahalanobis distance; and (3) identify optimal homozygous combinations for different environments via GGE biplot. By integrating univariate and multivariate analyses while correcting for family background, we provide a robust framework for marker-assisted selection in contrasting agro-ecological zones.

Methods

Plant material and population structure

The spring bread wheat population M17 originated from the cross between Chris Mutant (donor of *Rht-B1p*) and Novosibirskaya 67. Chris Mutant carried the semi-dwarfing allele *Rht-B1p*, the photoperiod-insensitive allele *Ppd-D1a*, the spring-habit allele *Vrn-A1a*, and the recessive alleles *vrn-B1* and *vrn-D1*. In contrast, Novosibirskaya 67 carried the wild-type tall-stature allele *Rht-B1a*, the photoperiod-sensitive allele *Ppd-D1b*, the spring-habit alleles *Vrn-A1a* and *Vrn-B1a*, and the recessive allele *vrn-D1*. Thus, the parental lines differed at three loci, and the M17 population segregated for *Rht-B1* (*Rht-B1a/Rht-B1p*), *Ppd-D1* (*Ppd-D1a/Ppd-D1b*), and *Vrn-B1* (*Vrn-B1a/vrn-B1*), whereas *Vrn-A1a* and *vrn-D1* were fixed in both parents. The initial $F_{3:4}$ families described in Kroupin et al. (2020) were further propagated by single-seed descent to $F_{4:5}$ and $F_{5:6}$ generations [6]. For the present study, 4107 individual plants (derived from 81 unique families) from these advanced generations were evaluated in field trials (referred to as M17). Detailed pedigree and allele characterization are given in Kroupin et al. (2020) [6].

Field experiments and environmental conditions

Field trials were conducted in five location–year environments:

- Krasnodar Krai, southern Russia (45°41' N, 38°55' E) – a region with a long growing season, short day length during early growth, and fertile chernozem soils. Sowing took place on 21 March 2018 and 25 March 2019.

- Moscow region, central Russia (55°50' N, 37°33' E) – a region with a short growing season, long photoperiod, and sod-podzolic soils. Sowing took place on 5 May 2018, 5 May 2019 and 12 May 2022.

In each environment, families were arranged in a randomised complete block design with three replications (two replications in Moscow 2022). Each plot consisted of a single row, 1 m long, with 30 cm spacing between rows and 50 cm between plots. Row length and seed density were adjusted to maintain a uniform stand of approximately 300 plants per m^2. Standard agronomic practices (weed control, pest and disease management) were applied without plant growth regulators. No additional nitrogen fertiliser was applied beyond the background level (100 kg N ha^{-1} as ammonium nitrate applied at GS 30–31).

Phenotyping

For each individual plant, the following traits were recorded on the main shoot in all five environments:

- Plant height (PH, cm) – distance from soil surface to the tip of the spike (excluding awns).
- Spike length (SL, cm) – from the base of the spike to the tip of the terminal spikelet.
- Grain number per spike (GNS) – counted manually after threshing.
- Grain weight per spike (GWS, g) – weight of all grains from the main spike.
- Calculated thousand-grain weight (cTGW, g) – calculated as (GWS / GNS) × 1000.
- Harvest index (HI) – ratio of grain weight to above-ground biomass of the main shoot. HI was calculated on the main shoot only; whole-plant HI may differ, especially in genotypes with contrasting tillering capacity
- Vegetative mass of the main spike (VMMS, g) – above-ground biomass excluding grain.
- Straw mass of the main spike (SMMS, g) – straw biomass of the main shoot.
- Spikelet number (SN) – number of spikelets per main spike.
- Spike density (SD) – calculated as (SN / SL) × 10.

The following traits were measured only in a subset of environments:

- Internode number (IN, count) – number of internodes in the main stem (Krasnodar 2018 and Moscow 2019).
- Days to heading (DH) – number of days from sowing to emergence of 50% of spikes (Zadoks scale 57) (Krasnodar 2018, Moscow 2019, Moscow 2022).
- Days to flowering (DF) – number of days from sowing to anthesis (Zadoks scale 65) (Moscow 2019, Moscow 2022).

A complete list of traits, their abbreviations, and the environments in which they were measured is provided in Supplementary Table S1 [see Additional file 1].

DNA extraction and allele calling

Genomic DNA was extracted from young leaves using a CTAB method [23]. Allele-specific PCR markers developed previously were used to genotype each family for *Rht-B1*, *Ppd-D1* and *Vrn-B1* [6]. For *Rht-B1*, two

allele-specific forward primers (Rht-B1p-F for the mutant and Rht-B1p-WF for the wild type) were used in separate PCR reactions with a common reverse primer (Rht-B1-R1). Both alleles yield a 425 bp amplicon, but the presence or absence of the specific fragment discriminates the alleles [5]. For *Ppd-D1*, the three-primer system Ppd-D1_F, Ppd-D1_R1 and Ppd-D1_R2 discriminated Ppd-D1a (288 bp) and *Ppd-D1b* (414 bp) [8]. For *Vrn-B1*, the marker Intr1/B/F and Intr1/B/R3 identified *Vrn-B1a* (709 bp) and *vrn-B1* (737 bp) [24]. PCR conditions and product visualisation were as described in Kroupin et al. (2020) [6].

Statistical analysis

All statistical analyses were performed in R version 4.6.1. The significance threshold was set at $\alpha = 0.05$. Inspection of the raw trait distributions revealed pronounced values at the distributional boundaries that were biologically implausible for the corresponding trait and environment and were therefore treated as likely data-entry anomalies. Accordingly, two-sided quantile trimming was applied separately within each environment–trait combination using the 5th and 95th percentiles as the lower and upper cutoffs; values outside these limits were replaced with NA. This quantile-based approach is robust to non-normal distributions and resulted in replacement of 6.6% of observations (3531 out of 53,391 individual trait records). The lower proportion reflects the presence of pre-existing missing data in some environment-trait combinations (e.g., DH and DF were not measured in all environments), which reduced the number of cells available for replacement.

Data preprocessing and exploratory analysis

Prior to formal testing, we performed an exploratory analysis to assess data quality and structure. For each environment, we examined the distribution of each trait using Shapiro–Wilk normality test [25]. For continuous traits, we applied transformation only when the absolute skewness exceeded 1.5. In the per-environment analysis, skewness values for all traits were below this threshold, so no transformation was applied. In the pooled dataset, SMMS exceeded the predefined skewness threshold; however, the primary mixed models were fitted to the original trait scale to preserve direct interpretability of the effect estimates. The count traits GNS, SN, DH, and DF were analysed using generalised linear mixed models as described in the environment-specific and pooled single-locus analyses. Internode number (IN) was treated as a continuous trait and analysed using a Gaussian linear mixed model.

To reduce multicollinearity and select informative traits for multivariate analyses, we performed principal component analysis (PCA) separately for each environment on standardised (Z-scored) traits, using the prcomp function [26]. Only traits with a squared cosine ($\cos^2$) ≥ 0.25 on the first two principal components were retained. The first two PCs explained 53.9–72.2% of total variance, depending on environment (Supplementary Table S2). This threshold corresponded to the elbow of the scree plot in each environment and ensured that all retained components captured meaningful multivariate structure [27]. We also removed traits with pairwise Spearman correlation $|\rho| \geq 0.85$, keeping the trait with higher $\cos^2$; this avoided redundancy from synthetic traits (e.g., cTGW derived from GWS and GNS). The threshold of 0.85 was chosen based on the elbow of the scree plot of eigenvalues from the correlation matrix; for each correlated pair, the trait with higher $\cos^2$ on PC1–PC2 was retained. The list of traits retained for each environment is provided in Supplementary Table S3.

Environment-specific single-locus effects

Single-locus effects were estimated separately within each of the five location–year environments. For each locus, two contrasting allele classes were compared. Throughout the manuscript, alleles are designated according to standard genetic nomenclature: *Rht-B1a* (tall stature) and *Rht-B1p* (semi-dwarfing); *Ppd-D1a* (photoperiod-insensitive) and *Ppd-D1b* (photoperiod-sensitive); and *Vrn-B1a* (spring habit) and *vrn-B1* (winter habit).

Only locus–environment combinations in which each allele class contained at least 10 observations from at least three families were analysed. For each trait and locus, allele class was included as a fixed effect and family as a random intercept. Continuous traits were analysed using Gaussian linear mixed models fitted by maximum likelihood with lmerTest::lmer, based on the lme4 framework [28]:

$$y_{ij} = \mu + A_i + F_j + \varepsilon_{ij}, \quad (\mathbf{1})$$

where (A_i) denotes allele class, (F_j) is the random family effect, and (ε_{ij}) is the residual error.

The count traits grain number per main spike (GNS), spikelet number (SN), days to heading (DH), and days to flowering (DF) were analysed using generalised linear mixed models with a Poisson distribution and log link, fitted with lme4::glmer [28]. Overdispersion was assessed as the sum of squared Pearson residuals divided by the residual degrees of freedom. When this ratio exceeded 1.4, the model was refitted using a negative-binomial distribution with the nbinom2 parameterisation in glmmTMB [29]. The number of internodes (IN) was treated as a continuous trait and analysed using a Gaussian LMM.

The overall effect of allele class was tested using a likelihood-ratio test comparing the full model with a reduced model containing only the random family intercept. For Gaussian LMMs, coefficient-level P-values were additionally obtained using Satterthwaite's approximation as implemented in lmerTest [30]. For GLMMs, coefficient-level P-values were based on Wald tests. The P-values used for multiple-testing correction were those obtained from the likelihood-ratio tests. To assess robustness of inference for count traits, we compared GLMM P-values with those from original-scale and rank-based Gaussian LMMs; the results are provided in Supplementary Table S4.

Because multiple traits were tested for each locus within each environment, Benjamini–Hochberg correction was applied separately within each locus–environment combination across traits. These local FDR-adjusted q-values were used as the primary significance criterion, with significance declared at $q < 0.05$. As a sensitivity analysis, we additionally applied Benjamini–Hochberg correction across all single-locus tests within each environment (global FDR). The two correction strategies produced broadly similar results, although several borderline effects changed significance status; the complete comparison is provided in Supplementary Table S5.

Pooled multi-environment single-locus effects

To estimate overall allele-class effects after accounting for environmental variation, observations from the five location–year environments were combined in pooled mixed models. For each trait and locus, the full model included allele class, location, year, and the location × year interaction as fixed effects, with family included as a random intercept:

$$y_{ijkl} = \mu + A_i + L_j + Y_k + (L\times Y)_{jk} + F_l + \varepsilon_{ijkl}, \quad (\mathbf{2})$$

where (A_i) denotes allele class, (L_j) denotes location, (Y_k) denotes year, (F_l) is the random family effect, and (ε_{ijkl}) is the residual error.

For DF, which was recorded only in Moscow in 2019 and 2022, a separate model was fitted to the Moscow observations with year as a fixed effect. For the remaining traits, the same distributional rules as in the environment-specific analyses described above were used. All pooled models were fitted to untransformed trait values.

Benjamini–Hochberg correction was applied separately for each locus across the traits included in the pooled analysis. The Moscow-only DF models formed a separate FDR-correction block. Statistical significance was declared at ($q < 0.05$).

Two-locus interactions

Pairwise interactions were tested for *Rht-B1 × Ppd-D1*, *Rht-B1 × Vrn-B1*, and *Ppd-D1 × Vrn-B1*. For each trait, a linear mixed model containing the main effects of both loci and their interaction was compared with an additive model containing only the two main effects. Family was included as a random intercept in both models. The models were fitted by maximum likelihood and compared using a likelihood-ratio test. The analyses were performed separately within each location–year environment and on the pooled dataset. In the pooled analysis, location, year, and the location × year interaction were included as additional fixed effects.

Likelihood-ratio tests were used to compare the nested models and assess interaction effects while accommodating the unbalanced structure of the data [32]. When the interaction was significant ($P < 0.05$ after FDR correction within each gene-pair), we performed post-hoc pairwise comparisons among the four analysed allele-class combinations using estimated marginal means (emmeans) with Tukey's adjustment for multiple comparisons [33]. Compact letter displays were generated using the multcomp package [34].

Family effect (ICC) and correction for relatedness

To quantify the proportion of phenotypic variance attributable to family structure, we calculated the intraclass correlation coefficient (ICC) from the environment-specific LMMs:

$$ICC = \sigma^2_{family} / (\sigma^2_{family} + \sigma^2_{residual})$$ [35] (**3**)

This coefficient ranges from 0 (no family effect) to 1 (all variance due to family). An ICC > 0.3 was considered moderate, and > 0.5 strong, indicating that family background must be accounted for to avoid spurious associations [21]. We also fitted ordinary least squares (OLS) models without the random family effect to compare with LMM results; divergence between OLS and LMM P-values indicated confounding by family structure.

Multivariate analyses

Principal component analysis

Principal component analysis was performed separately for each location–year environment using stats::prcomp. Traits with at least five non-missing observations were retained, and only observations with complete data for all retained traits were included. Each trait was centred and scaled to unit variance before

analysis. Environments with fewer than 10 complete observations or fewer than two analysable traits were excluded.

For the general informative-trait set used in the Python LDA and Mahalanobis analyses, a trait was retained when its maximum squared coordinate across the first four principal components, or across all available components when fewer than four were present, was at least 0.25. PCA plots stratified by locus were generated from observations belonging to the two analysed allele classes.

PERMANOVA

To test for multivariate differences between allele classes of each gene within each environment, we used permutational multivariate analysis of variance (PERMANOVA) [36], implemented with the adonis2 function of the vegan package [37]. The analysis was performed on the Euclidean distance matrix derived from standardised informative traits (selected during data preprocessing and exploratory analysis). Multicollinearity among the retained traits was assessed using variance inflation factors (VIF) calculated from linear models; all VIF values were below 5, indicating acceptable levels of collinearity. All PERMANOVA tests were performed using unstratified permutations (999 iterations), because allele classes were constant within families, making stratified permutations ineffective. We also examined homogeneity of multivariate dispersions using the betadisper function [36] to test whether significant PERMANOVA results could be driven by differences in variance rather than centroids.

Mahalanobis distance and Hotelling's T^2

For each environment and locus, the squared Mahalanobis distance (D^2) between the two allele-class centroids was calculated using the pooled within-group covariance matrix and its Moore–Penrose pseudoinverse [38]. Hotelling's T^2 was obtained as

$$T^2 = (n_1 n_2 / (n_1+n_2))\, D^2 \quad (4)$$

$$F = T^2 \times (n_1 + n_2 - p - 1) / ((n_1 + n_2 - 2) \times p),$$

and the corresponding P-value was obtained from the F distribution with numerator degrees of freedom p and denominator degrees of freedom $n_1 + n_2 - p - 1$, where p is the number of traits retained for that comparison [39].

Canonical variate analysis / linear discriminant analysis (CVA/LDA)

Linear discriminant analysis was used to quantify the multivariate separation between the two analysed allele classes for each locus and environment. The analysis was implemented in Python using scikit-learn's LinearDiscriminantAnalysis on the informative-trait matrix (numeric trait values without additional within-function standardisation). Classification performance was evaluated using five-fold stratified cross-validation, with the number of folds reduced when necessary so that it did not exceed the size of the smaller allele class. Mean classification accuracy and its standard deviation were calculated across the cross-validation folds. Discriminant coefficients were not exported as a primary analysis output.

GGE biplot

Genotype × environment (GGE) biplot was constructed for grain weight per spike using the four homozygous combinations of *Rht-B1* and *Ppd-D1*. For each combination, we computed the mean GWS in each environment. The data were centred by environment (subtracting environment means), and singular value decomposition was performed on the centred matrix. Projections of genotypes onto environment vectors were computed as the scalar product of genotype and environment coordinates; this preserves the relative ranking of genotypes within each environment. Because the axes are scaled consistently across the biplot, comparisons of projections between different environments are meaningful only within the same biplot. The first two principal components were plotted as a biplot, with genotypes as points and environments as vectors [22]. The angles between environment vectors indicate correlations between environments; genotypes with a high projection onto an environment vector are best adapted to that environment.

Correlation analyses

Spearman rank correlation coefficients were calculated between all pairs of traits within each environment using the cor.test function. Spearman correlation was chosen because it does not assume normality and is robust to outliers [41]. Heatmaps with hierarchical clustering (Ward's method) were produced using the corrplot package [42] to visualise the correlation structure.

Software and reproducibility

The analysis-ready dataset, full statistical outputs, and executable analysis code are provided in Additional files 2–5.

Most statistical analyses were performed in R using tidyverse for data manipulation; ggplot2 and plotly for graphical visualisation; lme4 and lmerTest for linear mixed models; glmmTMB for generalised linear mixed models; emmeans and multcomp for post-hoc comparisons; vegan for PERMANOVA; stats::prcomp for PCA; corrplot for correlation-matrix visualisation; and factoextra for PCA visualisation. Package versions were not pinned in an environment lockfile for this submission package.

Additional multivariate analyses were implemented in Python. Data import, preprocessing, grouping, and tabular output were performed using pandas and NumPy. Linear discriminant analysis was performed using scikit-learn's LinearDiscriminantAnalysis and evaluated by five-fold stratified cross-validation (sklearn.model_selection.cross_val_score). Squared Mahalanobis distances between allele-group centroids were calculated from pooled within-group covariance matrices using NumPy (including np.linalg.pinv), and the corresponding Hotelling's T^2 statistics and F-distribution-based P-values were calculated using SciPy. HTML reports were generated using Jinja2, and interactive visualisations were produced using Plotly. Full statistical outputs are provided in Additional files 2 and 3, the analysis-ready dataset in Additional file 4, and the analysis code in Additional file 5.

Results

Data overview and balance

After quality control and replacement of outlier values with missing values, the final dataset comprised 4107 individual plants derived from 81 families across five location–year environments. Both analysed allele classes

were represented for each locus in every environment, although their frequencies varied among loci and location–year combinations (Supplementary Table S6). Differences in total plant numbers among loci within the same environment reflected missing genotype information for some individuals.

Single-gene effects

Rht-B1

The semi-dwarf allele *Rht-B1p* exhibited the most consistent and strongest effects across all environments. In univariate analyses (LMM/GLMM with family as random effect and allele as fixed effect, FDR-corrected $q < 0.05$), significant effects were observed for plant height (PH) in all five environments ($q < 0.001$), with height reduction ranging from 18.4 cm (Moscow 2018) to 38.3 cm (Krasnodar 2019), corresponding to a 25–36% decrease relative to the tall allele (Table 1, Fig. 1).

Table 1
Matrix of significant single-locus effects across traits and environments

Trait	*Ppd-D1*	*Rht-B1*	*Vrn-B1*
Phenology			
DH	K18 ↑0.079*** (RR 1.083) M19 ↑0.055*** (RR 1.057) M22 ↑0.049*** (RR 1.050)	M22 ↑0.037** (RR 1.038)	—
DF	M19 ↑0.049** (RR 1.051) M22 ↑0.019* (RR 1.020)	M19 ↑0.046** (RR 1.047)	—
Plant architecture			
PH	K19 ↑1.9*** M19 ↑5.045** M22 ↓-2.748**	K18 ↓-27.249*** K19 ↓-38.332*** M18 ↓-18.371*** M19 ↓-24.494*** M22 ↓-24.499***	K19 ↓-2.734** M22 ↓-3.418*
IN	—	K18 ↓-0.411*** M19 ↓-0.348***	—
SL	K19 ↑0.657*** M22 ↑0.354***	—	—
SD	M19 ↑0.913**	—	—
SN	M22 ↑0.054** (RR 1.055)	—	—
Yield components and biomass			
GNS	K19 ↑0.091*** (RR 1.095) M19 ↑0.07** (RR 1.072)	—	K19 ↓-0.088*** (RR 0.915)
GWS	K19 ↑0.127** M19 ↑0.097*	K18 ↓-0.107** K19 ↓-0.287*** M18 ↑0.177***	K19 ↓-0.086*
cTGW	—	K18 ↓-2.75*** K19 ↓-6.464*** M18 ↓-4.188*** M19 ↑1.123* M22 ↓-1.881**	—

Trait	*Ppd-D1*	*Rht-B1*	*Vrn-B1*
Phenology			
SMMS	K19 ↑0.171**	K18 ↓-0.598***	K19 ↓-0.113**
	M19 ↑0.063*	K19 ↓-0.305***	
		M18 ↓-0.227***	
		M19 ↑0.263***	
		M22 ↑0.228***	
VMMS	K19 ↑0.635***	K18 ↓-0.109*	K19 ↓-0.168*
	M19 ↑0.114*	K19 ↓-1.003***	
	M22 ↑0.103*	M18 ↓-0.208***	
HI	K19 ↓-0.017***	K18 ↑0.015***	M22 ↓-0.017*
		M18 ↑0.019***	
		M19 ↑0.048***	
		M22 ↑0.057***	

Note. Only effects significant after Benjamini–Hochberg correction are shown. Arrows indicate the direction of the effect. Effect sizes are model coefficients; RR denotes the rate ratio for count traits. Significance levels: * q < 0.001, ** q < 0.01, and * q < 0.05. Contrasts: Ppd-D1b versus Ppd-D1a; Rht-B1p versus Rht-B1a; and Vrn-B1a versus vrn-B1. Environment abbreviations: K18, Krasnodar 2018; K19, Krasnodar 2019; M18, Moscow 2018; M19, Moscow 2019; M22, Moscow 2022. Significance is based on Benjamini–Hochberg correction applied within each locus–environment combination across traits.**

The effect of the semi-dwarfing Rht-B1p allele on calculated thousand-grain weight (cTGW) was significant in all five environments but varied in direction. cTGW decreased in Krasnodar 2018 and 2019 and Moscow 2018 and 2022, whereas a small increase was observed in Moscow 2019 (Table 1). Grain weight per main spike (GWS) decreased in Krasnodar 2018 and 2019 but increased in Moscow 2018; no significant effect was detected in Moscow 2019 or Moscow 2022. Vegetative mass of the main spike (VMMS) decreased in Krasnodar 2018 and 2019 and Moscow 2018, with no significant effects in Moscow 2019 or Moscow 2022. Straw mass of the main spike (SMMS) decreased in Krasnodar 2018 and 2019 and Moscow 2018 but increased in Moscow 2019 and Moscow 2022. Harvest index (HI) was significantly increased by the Rht B1p allele in four out of five environments (Krasnodar 2018, Moscow 2018, Moscow 2019, Moscow 2022; $q < 0.05$), with no significant effect in Krasnodar 2019. Phenology traits (DH and DF) were affected in Moscow 2019 (DF only, $q = 0.007$), where the Rht B1p allele delayed flowering by 2.4 days (rate ratio = 1.047, corresponding to a 4.7% increase, GLMM log link coefficient = 0.046, q = 0.007) and in Moscow 2022 (DH only, $q = 0.001$), where the Rht-B1p allele delayed heading by 2.0 days (GLMM log link coefficient = 0.037). No significant effects were detected for spikelet number (SN), grain number per spike (GNS), spike length (SL) or spike density (SD) in any environment. Internode number (IN) was significantly reduced in Krasnodar 2018 and Moscow 2019 ($q < 0.05$, Table 1). The pooled analysis (environment as fixed effect model) confirmed the robustness of the effects on PH, cTGW, GWS, VMMS, SMMS and HI, with estimates consistent with the per environment results. The gene estimate for

PH in the pooled model was −24.5 cm (p ≈ 5.4e 46), closely matching the average of per environment estimates. Ppd D1 The photoperiod-sensitive allele Ppd-D1b showed significant effects in a subset of environments (Table 1). In Krasnodar 2019, Ppd-D1b increased plant height by 1.9 cm based on the family-adjusted estimated marginal means. The overall Ppd-D1 effect on plant height remained significant after FDR correction ($q = 1.71 \times 10^{-8}$). The raw difference between the allele-class means was also approximately 1.9 cm, whereas the corresponding linear mixed-model fixed-effect coefficient (model with family as a random intercept) was 11.1 cm. This discrepancy was consistent with strong family confounding (ICC = 0.95 in this environment), because tall and short families were unevenly distributed between the Ppd-D1 allele classes. The estimate reported in Table 1 is the 1.9 cm value. The quoted q-value refers to the overall likelihood-ratio test of the Ppd-D1 effect and not to a separate test of the estimated-marginal-mean contrast. In the same environment, Ppd-D1b increased grain weight per main spike (GWS), vegetative mass of the main spike (VMMS), and straw mass of the main spike (SMMS), while decreasing harvest index (HI). Spike length increased by 0.66 cm in Krasnodar 2019 ($q = 4.2 \times 10^{-6}$) and by 0.35 cm in Moscow 2022 ($q = 5.8 \times 10^{-5}$). In Moscow 2019, Ppd-D1b increased grain number per main spike (GNS; q = 0.0018), GWS (q = 0.016), VMMS (q = 0.016), SMMS (q = 0.043), spike density (SD; q < 0.05), and plant height by 5.0 cm ($q = 1.3 \times 10^{-3}$). No significant effect on spike length was detected in Moscow 2019 (q = 0.237). In Moscow 2022, Ppd-D1b reduced plant height by 2.7 cm (q = 0.001) and affected both days to heading and days to flowering (q < 0.05). It also increased spikelet number and vegetative mass of the main spike, whereas its effects on grain number and grain weight per main spike did not reach the FDR threshold. No significant single-locus effects of Ppd-D1 were detected in Moscow 2018. In Krasnodar 2018, Ppd-D1b delayed heading, with a GLMM log-link coefficient of 0.079 ($q = 3.0 \times 10^{-6}$), corresponding to an observed difference of approximately 5.3 days between the raw allele-class means (69.9 versus 64.6 days). Across the Moscow environments, Ppd-D1b delayed heading by approximately 2–3 days and flowering by approximately 1.1–2.7 days (all q < 0.05). Although statistically significant, these shifts were modest and close to the temporal resolution of the field observations. Their agronomic relevance is therefore uncertain, particularly in Moscow 2022, where the phenological shift was not accompanied by a significant single-locus effect on GWS. A larger delay of approximately five days was observed in Krasnodar 2018, whereas no significant phenological effect was detected in Krasnodar 2019.

Vrn-B1

The spring allele *Vrn-B1a* showed the weakest and least consistent effects among the three genes (Table 1). Significant single-gene effects were detected in only 7 trait-environment combinations. In Krasnodar 2019, the *Vrn-B1a* allele significantly reduced plant height by 2.7 cm (q = 0.0087), decreased GWS, VMMS, SMMS and GNS (q < 0.05). In Moscow 2022, the *Vrn-B1a* allele significantly reduced plant height (q = 0.010) and harvest index (q = 0.029). In Moscow 2019, trends for cTGW and HI did not reach the q < 0.05 threshold. In Krasnodar 2019, the *Vrn-B1a* allele also decreased VMMS (q = 0.045, Table 1). In pooled analysis, only PH, HI, VMMS and GNS retained significance, and the effect sizes were small. No effects were observed on phenology traits (DH, DF) in any environment, consistent with the presence of the dominant *Vrn-A1a* allele, which is epistatic to *vrn-B1* [16, 17].

Two-locus interactions

Likelihood-ratio tests identified significant two-locus interactions at an FDR-adjusted threshold of $q < 0.05$, with most environment-specific effects detected in Krasnodar 2019 and Moscow 2019 and 2022 (Fig. 2A; Supplementary Table S7). Pooled multi-environment analyses further identified interaction effects that remained significant across environments (Fig. 2B). Representative crossover interactions are shown for the Ppd-D1 × Vrn-B1 effects on calculated thousand-grain weight in Moscow 2022 (Fig. 2C) and grain weight per main spike in Krasnodar 2019 (Fig. 2D).

Likelihood-ratio tests followed by Benjamini–Hochberg FDR correction identified the broadest interaction effects for *Ppd-D1 × Vrn-B1*. Significant environment-specific effects were detected for 12 trait–environment combinations, involving phenology, spike morphology, biomass, and grain-weight traits in Krasnodar 2019 and Moscow 2019 and 2022. In the pooled analysis, this interaction remained significant for GWS, cTGW, SL, VMMS, SD, and DH. The *Rht-B1 × Ppd-D1* interaction also showed both environment-specific and pooled effects, with significant cross-environment associations for PH, SMMS, and DH. By contrast, *Rht-B1 × Vrn-B1* was significant only in individual environments and showed no pooled effects after FDR correction, indicating strong environmental specificity.

The interaction patterns differed between environments and traits. In Moscow 2022, the effect of Ppd-D1 on cTGW depended on the Vrn-B1 allelic background (Fig. 2C), whereas a distinct non-additive pattern was observed for GWS in Krasnodar 2019 (Fig. 2D).

Multivariate analyses

PCA and trait selection

After PCA-based filtering and correlation pruning, 6–10 informative traits were retained per environment (Supplementary Table S3). Depending on the environment, one of several strongly correlated biomass or grain-weight traits was removed to reduce redundancy.

PERMANOVA

PERMANOVA (Euclidean distance, unstratified permutations) revealed significant multivariate differences between allele classes for all three genes in most environments, but with markedly different effect sizes (Table 2).

Table 2
Summary of PERMANOVA, linear discriminant analysis, and Mahalanobis-distance results by environment and gene

Environment	Gene	PERMANOVA R^2	PERMANOVA P	n	LDA accuracy	Mahalanobis D^2	Mahalanobis P
Krasnodar 2018	*Rht-B1*	0.161	0.001	416	0.998	39.32	< 0.001
Krasnodar 2018	*Ppd-D1*	0.049	0.001	404	0.664	0.61	< 0.001
Krasnodar 2018	*VRN-B1*	0.007	0.017	416	0.544	0.22	0.032
Krasnodar 2019	*Rht-B1*	0.367	0.001	550	0.996	47.83	< 0.001
Krasnodar 2019	*Ppd-D1*	0.032	0.001	550	0.739	1.69	< 0.001
Krasnodar 2019	*VRN-B1*	0.030	0.001	550	0.667	1.02	< 0.001
Moscow 2018	*Rht-B1*	0.155	0.001	643	0.894	6.82	< 0.001
Moscow 2018	*Ppd-D1*	0.007	0.007	599	0.618	0.38	< 0.001
Moscow 2018	*VRN-B1*	0.001	0.476	643	0.664	0.08	0.456
Moscow 2019	*Rht-B1*	0.214	0.001	351	0.951	16.74	< 0.001
Moscow 2019	*Ppd-D1*	0.036	0.010	351	0.817	3.20	< 0.001
Moscow 2019	*VRN-B1*	0.013	0.126	351	0.698	1.07	< 0.001†
Moscow 2022	*Rht-B1*	0.227	0.001	601	0.998	27.38	< 0.001
Moscow 2022	*Ppd-D1*	0.092	0.001	601	0.780	3.05	< 0.001
Moscow 2022	*VRN-B1*	0.006	0.001	601	0.576	0.35	< 0.001

Notes: PERMANOVA R^2 and P values were obtained using adonis; n, number of observations included in the analysis; LDA, linear discriminant analysis. Mahalanobis D^2 denotes the squared distance between allele-group centroids. † Interpret with caution because the betadisper test was significant ($P < 0.05$), indicating heterogeneous multivariate dispersions; the Mahalanobis D^2 value may therefore partly reflect differences in dispersion rather than only a shift in group centroids.

Rht B1 and Ppd-D1 was significant in all five environments (R2 = 0.155–0.367 and R2 = 0.007–0.092, respectively). vrn B1 was significant in Krasnodar 2018, Krasnodar 2019 and Moscow 2022 ($p < 0.05$), but not in Moscow 2018 ($p = 0.476$) and 2019 ($p = 0.126$).

Canonical variate analysis (CVA/LDA)

LDA cross-validation accuracy clearly ranked the genes (Table 2):

- *Rht-B1*: 0.894–0.998 (mean 0.967)
- *Ppd-D1*: 0.618–0.817 (mean 0.723)
- *VRN-B1*: 0.544–0.698 (mean 0.630)

For *Rht-B1*, plant height (PH) was the primary trait contributing to discrimination, consistent with the direct effect of the semi-dwarfing allele *Rht-B1p* on plant stature. Nevertheless, cTGW, VMMS, and several other traits also contributed to the discriminant function. Thus, the high LDA classification accuracy of 96.7% reflected a broader pleiotropic phenotypic signature rather than separation based solely on plant height.

Mahalanobis distance and Hotelling's T2

Mahalanobis distances (D^2) confirmed the hierarchy (Table 2). *Rht-B1* D^2 values were substantially larger than those for *Ppd-D1* (0.38–3.20) and *vrn-B1* (0.076–1.015). All *Rht-B1* distances were highly significant; *vrn-B1* D^2 was non-significant in Moscow 2018 ($p = 0.456$). For *Vrn-B1* in Moscow 2019, PERMANOVA was not significant ($p = 0.126$).

Family effect (ICC) and correction for relatedness

ICC values varied substantially among traits and loci (Supplementary Table S8). For plant height, family effects were strongest in the Ppd-D1 and Vrn-B1 analyses, with mean ICC values of approximately 0.86 across environments, whereas the mean ICC for Rht-B1 was approximately 0.35. For most other traits, mean ICC values ranged from approximately 0.15 to 0.49, although individual environment-specific estimates reached approximately 0.71. These results indicate that the contribution of family background depended strongly on both the analysed trait and locus. The maximum ICC was 0.95 for plant height in the Ppd-D1 analysis in Krasnodar 2019.

GGE biplot for Rht-B1 × Ppd-D1 combinations

GGE biplot for grain weight per spike (GWS) captured 99.8% of G×E variance (PC1 82.8%, PC2 17.0%; Fig. 3). Numerical allele-combination coordinates, environment coordinates, and projection values are provided in Supplementary Table S9.

Genotype stability was assessed using the coefficient of variation (CV) of grain weight per main spike (GWS) across five environments (Supplementary Table S10). The tall combinations Rht-B1a/Ppd-D1a and Rht-B1a/Ppd-D1b were more stable (11.6% and 14.4%) than the semi-dwarfing combinations Rht-B1p/Ppd-D1a and Rht-B1p/Ppd-D1b (20.4% and 21.8%) (Supplementary Table S10).

In Moscow 2022, Rht-B1a/Ppd-D1b showed the highest GWS and largest positive projection, whereas Rht-B1p/Ppd-D1b combined similar productivity with reduced stature and a high harvest index. Rht-B1a/Ppd-D1a was more closely associated with Krasnodar 2019, indicating substantial genotype × environment interaction. These patterns are descriptive because genotype means were not formally compared within environments. Numerical projection values are provided in Supplementary Table S9.

Correlation structure and PCA

Spearman correlations (Supplementary Figure S1) showed strong positive associations among yield-related traits (GWS, cTGW, GNS, VMMS) and negative correlations between PH and HI in Moscow ($\rho \approx -0.45$ to -0.65). Phenology traits correlated negatively with cTGW and GWS. Trait-correlation patterns varied among location–year environments (Supplementary Figure S1).

Summary of gene effects and environment specificity

Among the three loci, *Rht-B1* showed the strongest and most stable effects, with *Rht-B1p* influencing plant height and several productivity-related traits. The effects of *Ppd-D1b* were more environment-dependent, whereas *Vrn-B1* had only limited effects in the fixed *Vrn-A1a* background. The *Ppd-D1 × Vrn-B1* interaction was the most consistent two-locus effect, while *Rht-B1 × Ppd-D1* affected fewer traits and *Rht-B1 × Vrn-B1* was mainly environment-specific. Strong family effects for *Ppd-D1* and *Vrn-B1* further highlighted the need to account for relatedness in mixed models.

Discussion

Single-gene effects

Rht-B1p: a strong and stable semi-dwarfing allele

Among the three loci examined, *Rht-B1* produced the strongest and most consistent phenotypic signal across environments and analytical approaches. The semi-dwarfing allele *Rht-B1p* reduced plant height by 18–38 cm across all five environments, and this effect remained highly significant after adjustment for family structure. The magnitude of height reduction was comparable to that reported for other gibberellin-insensitive dwarfing alleles, including the widely used *Rht-B1b* and *Rht-D1b* alleles [2, 4, 43]. These findings support the potential of *Rht-B1p* as an additional source of semi-dwarfism for wheat breeding.

The broad phenotypic influence of *Rht-B1p* is consistent with the regulatory role of DELLA proteins in gibberellin signalling. In addition to controlling cell elongation, DELLA-mediated pathways influence assimilate partitioning, reproductive development, and grain formation. Previous studies have similarly shown that major height loci may account for a substantial proportion of variation in plant architecture while also exerting pleiotropic effects on biomass and yield components [44]. The stability of the height response observed here therefore distinguishes *Rht-B1p* from the more environmentally conditional effects of the photoperiod and vernalisation loci.

Ppd-D1b: environment-dependent effects on phenology and productivity

The effects of the photoperiod-sensitive allele *Ppd-D1b* were concentrated in Krasnodar 2019 and Moscow 2019 and 2022, indicating pronounced environmental dependence. *Ppd-D1b* delayed heading and flowering, altered plant height, and affected spike morphology, biomass, and several yield components. This broad but variable response agrees with previous evidence that *Ppd-D1* regulates not only flowering time but also plant height, spike development, biomass accumulation, and yield formation, with effect sizes depending strongly on environmental and genetic context [10, 12, 45, 46].

The effects of *Ppd-D1b* were strongly environment-dependent. In Moscow, the allele delayed heading by 2–3 days and flowering by 1.1–2.7 days, but these modest shifts did not consistently improve grain productivity; in Moscow 2022, neither GNS nor GWS increased significantly after FDR correction. Heading was delayed by approximately five days in Krasnodar 2018, whereas no phenological effect was detected in Krasnodar 2019.

Yield-related effects were likewise inconsistent. *Ppd-D1b* increased several spike and biomass traits in Krasnodar 2019 and Moscow 2019, and increased spike length or spikelet number in Moscow 2022, but comparable yield benefits were absent in that environment. Plant-height responses also varied: after family adjustment, the allele increased height by 1.9 cm in Krasnodar 2019 and 5.0 cm in Moscow 2019 but reduced it by 2.7 cm in Moscow 2022. The discrepancy between unadjusted and family-adjusted estimates in Krasnodar 2019 further showed that part of the apparent effect reflected family confounding. Overall, *Ppd-D1b* had biologically relevant but substantially more environment- and background-dependent effects than *Rht-B1p*.

Vrn-B1: limited marginal effects in a fixed Vrn-A1a background

The marginal effects of *Vrn-B1* were weaker and less consistent than those of *Rht-B1* and *Ppd-D1*. Significant differences between *Vrn-B1a* and *vrn-B1* were detected mainly in Krasnodar 2019 and Moscow 2022 and involved a restricted set of productivity, biomass, and plant-height traits. No consistent effect on heading or flowering time was observed.

This limited response should be interpreted in the context of the fixed *Vrn-A1a* background of the M17 population. *Vrn-A1* is generally a stronger determinant of spring growth habit than *Vrn-B1*, and its presence can mask or reduce the phenological effects of other vernalisation loci [16, 47]. The absence of a strong marginal *Vrn-B1* effect therefore does not indicate that this locus is universally neutral. Studies in other genetic backgrounds have demonstrated that variation at *Vrn-B1* may alter heading time, yield, and other agronomic traits, particularly when the effect of *Vrn-A1* is absent or less dominant [48, 49].

Our findings suggest that, in spring wheat already carrying *Vrn-A1a*, direct selection at *Vrn-B1* is unlikely to generate a large and stable phenotypic response. However, the significant interactions involving *Vrn-B1* indicate that the locus retains functional effects that become detectable in specific photoperiodic and environmental contexts.

Two-way interactions

The *Ppd-D1 × Vrn-B1* interaction affected the broadest range of traits and showed the greatest consistency across environments. Significant environment-specific effects were detected for phenology, grain weight, harvest index, spike morphology, and biomass, and pooled effects remained significant for DH, GWS, cTGW, SL, VMMS, and SD. These findings support non-additive regulation between the photoperiod and vernalisation

pathways. Interactions between *Ppd-1* and *Vrn-1* alleles have also been reported in other wheat populations, where the effect of a vernalisation allele depended on photoperiod sensitivity and environmental conditions [45, 47, 50].

The *Ppd-D1 × Vrn-B1* interaction was notable because *Vrn-B1* showed only weak marginal effects in the fixed *Vrn-A1a* background. Its crossover effects on cTGW and GWS suggest that *Vrn-B1* retained context-dependent activity that became evident through interaction with *Ppd-D1*. The *Rht-B1 × Ppd-D1* interaction was less extensive but remained significant for PH, SMMS, and DH in the pooled analysis, indicating joint effects on development and biomass allocation. By contrast, *Rht-B1 × Vrn-B1* was confined to individual environments. Thus, *Ppd-D1 × Vrn-B1* was the most broadly supported interaction, although pooled *Rht-B1 × Ppd-D1* effects also contributed to phenotypic variation.

Multivariate analyses

Multivariate analyses confirmed the single-trait results. *Rht-B1* was the strongest discriminator, with 96.7% LDA accuracy, large Mahalanobis distances, and a substantial PERMANOVA effect. Although plant height dominated the separation, cTGW, VMMS, and other traits indicated a broader pleiotropic signature of *Rht-B1p*. *Ppd-D1* showed moderate discrimination, whereas *Vrn-B1* produced weak separation in the fixed *Vrn-A1a* background. This contrast is consistent with the broad developmental role of the DELLA regulator *Rht-B1* and the more specific, background-dependent function of *Vrn-B1*. Multivariate phenotyping may therefore support preliminary identification of *Rht-B1p* carriers, but it should complement rather than replace molecular genotyping because the classifier was evaluated in a single population.

Family effect

Family background strongly influenced several locus–trait associations, with ICC values for plant height reaching 0.95 in the *Ppd-D1* analysis. By contrast, the effect of *Rht-B1p* remained large after family adjustment. In Krasnodar 2019, the unequal distribution of *Ppd-D1* alleles among tall and short families inflated unadjusted estimates, whereas mixed models produced smaller family-corrected effects. These findings show that allele effects in biparental populations may be confounded by relatedness when major and moderate-effect loci are unevenly distributed among families [44]. Modelling family as a random effect was therefore essential for separating focal-locus effects from genetic background.

GGE biplot and breeding implications

The GGE biplot showed environment-dependent performance of *Rht-B1 × Ppd-D1* allele combinations. In Moscow 2022, *Rht-B1a/Ppd-D1b* had the highest GWS and strongest positive projection, whereas *Rht-B1p/Ppd-D1b* combined similar productivity with reduced stature and a high harvest index. *Rht-B1a/Ppd-D1a* performed relatively poorly in Moscow 2022 but was more closely associated with Krasnodar 2019. Although the tall combinations were more stable across environments, *Rht-B1a/Ppd-D1b* was preferable for maximum spike productivity, while *Rht-B1p/Ppd-D1b* offered the best compromise between height reduction and yield. Because lodging was not measured, any lodging-resistance advantage remains inferential.

Limitations and future directions

The main limitation of this study is the use of a single biparental population and an unbalanced set of environments, which may restrict the generality of the detected allele and interaction effects. Family relatedness was modelled only through a random intercept, while pedigree- or marker-based relationship matrices would provide more precise adjustment. Lodging, grain quality, and other end-use traits were not measured, and independent multi-environment validation is therefore required. Nevertheless, the combined mixed-model, interaction, multivariate, and GGE framework effectively distinguished stable locus effects from environment- and background-dependent responses.

Conclusions

1. *Rht-B1p* is the strongest and most stable discriminator among the three genes, consistently reducing height by 25–36% and significantly affecting yield components. Its multivariate discriminatory power (mean LDA accuracy 96.7%) far exceeds that of *Ppd-D1b* and *vrn-B1*.
2. *Ppd-D1b* shows environment-specific effects on phenology and yield, with a moderate multivariate signal. The interaction *Ppd-D1* × *vrn-B1* is the most stable epistatic interaction.
3. *vrn-B1* had minor, environment-specific effects in the *Vrn-A1a* background, confirming its redundancy for spring wheat breeding.
4. Family structure must be accounted for to obtain unbiased estimates, especially for *Ppd-D1b* and *vrn-B1* whose effects were strongly influenced by family background.
5. Multivariate methods provide a robust framework for dissecting pleiotropy and G×E interactions.

Abbreviations

cTGW
calculated thousand-grain weight
CV
coefficient of variation
DF
days to flowering
DH
days to heading
FDR
false discovery rate
GGE
genotype plus genotype-by-environment
GLMM
generalized linear mixed model
GNS
grain number per main spike
GWS
grain weight per main spike
HI
harvest index

ICC
intraclass correlation coefficient
IN
internode number
LDA
linear discriminant analysis
LMM
linear mixed model
OLS
ordinary least squares
PCA
principal component analysis
PERMANOVA
permutational multivariate analysis of variance
PH
plant height
SD
spike density
SL
spike length
SMMS
straw mass per main spike
SN
spikelet number
VMMS
vegetative mass of the main spike.

Declarations

Competing interests

The authors declare that they have no competing interests.

Funding

This research was funded by the Ministry of Science and Higher Education of the Russian Federation (the Federal Scientific-technical program for genetic technologies development for 2019–2030, agreement N 075-15-2025-480)

Authors' contributions

P.K.: Conceptualization, Methodology, Formal analysis, Writing - original draft, Writing -review & editing, Visualization, Investigation, Supervision. **L.N.:** Conceptualization, Methodology, Formal analysis, Data curation,

Investigation, Validation. **V.P.**: Conceptualization, Data curation, Resources. **V.V.**: Data curation, Formal analysis, Investigation, Methodology, Software, Visualization, Writing - original draft, Writing - review & editing. **L.B.**: Conceptualization, Investigation, Data curation, Supervision, Resources. **A.Ch.**: Conceptualization, Methodology, Formal analysis, Data curation, Investigation, Supervision, Validation, Writing - review & editing. **A.K.**: Data curation, Investigation, Methodology. **G.K.**: Funding acquisition, Supervision. **M.G.**: Conceptualization, Funding acquisition, Investigation, Methodology, Project administration, Resources, Supervision, Validation, Writing - review & editing.

Use of generative AI and AI-assisted technologies

During the preparation of this manuscript, the authors used ChatGPT (OpenAI) and Cursor Agent to assist with language editing and code review. All AI-generated suggestions were critically evaluated, verified, and revised by the authors. The authors take full responsibility for the accuracy, integrity, and final content of the article.

References

1. Casebow R, Hadley C, Uppal R, Addisu M, Loddo S, Kowalski A, Griffiths S, Gooding M. Reduced Height (Rht) Alleles Affect Wheat Grain Quality. PLoS ONE. 2016;11:e0156056. https://doi.org/10.1371/journal.pone.0156056.
2. Jobson EM, Johnston RE, Oiestad AJ, Martin JM, Giroux MJ. The Impact of the Wheat Rht-B1b Semi-Dwarfing Allele on Photosynthesis and Seed Development Under Field Conditions, Front. Plant Sci. 2019;10:51. https://doi.org/10.3389/fpls.2019.00051.
3. Xu D, Hao Q, Yang T, et al. Impact of Green Revolution gene Rht-B1b on coleoptile length of wheat. Front Plant Sci. 2023;14:1147019. https://doi.org/10.3389/fpls.2023.1147019.
4. Flintham JE, Börner A, Worland AJ, Gale MD. Optimizing wheat grain yield: effects of *Rht*(gibberellin-insensitive) dwarfing genes. J Agric Sci. 1997;128:11–25. https://doi.org/10.1017/S0021859696003942.
5. Bazhenov MS, Divashuk MG, Amagai Y, Watanabe N, Karlov GI. Isolation of the dwarfing Rht-B1p (Rht17) gene from wheat and the development of an allele-specific PCR marker. Mol Breed. 2015;35:1–8. https://doi.org/10.1007/s11032-015-0407-1.
6. Kroupin PY, Karlov GI, Bespalova LA, Salina EA, Chernook AG, Watanabe N, Bazhenov MS, Panchenko VV, Nazarova LA, Kovtunenko VY, Divashuk MG. Effects of Rht17 in combination with Vrn-B1 and Ppd-D1 alleles on agronomic traits in wheat in black earth and non-black earth regions. BMC Plant Biol. 2020;20:304. https://doi.org/10.1186/s12870-020-02514-0.
7. Gasperini D, Greenland A, Hedden P, Dreos R, Harwood W, Griffiths S. Quantification of the effects of VRN1 and Ppd-D1 to predict spring wheat (Triticum aestivum) heading time across diverse environments. J Exp Bot. 2014;65:6760–6760. https://doi.org/10.1093/jxb/ers138.
8. Beales J, Turner A, Griffiths S, Snape JW, Laurie DA. A Pseudo-Response Regulator is misexpressed in the photoperiod insensitive Ppd-D1a mutant of wheat (Triticum aestivum L). Theor Appl Genet. 2007;115:721–33. https://doi.org/10.1007/s00122-007-0603-4.
9. Zheng B, Biddulph B, Li D, Kuchel H, Chapman S. Quantification of the effects of VRN1 and Ppd-D1 on developmental and agronomic traits in wheat. J Exp Bot. 2013;64:5267–77.

https://doi.org/10.1093/jxb/ert209.

10. Morgounov A, Babkenov A, Ben C, Chudinov V, Dolinny Y, Dreisigacker S, Fedorenko E, Gentzbittel L, Rasheed A, Savin T, Shepelev S, Zhapayev R, Shamanin V. Molecular Markers Help with Breeding for Agronomic Traits of Spring Wheat in Kazakhstan and Siberia. Genes. 2024;15:86. https://doi.org/10.3390/genes15010086.
11. Worland AJ, Börner A, Korzun V, Li WM, Petrovíc S, Sayers EJ. The influence of photoperiod genes on the adaptability of European winter wheats. Euphytica. 1998;100:385–94. https://doi.org/10.1023/A:1018327700985.
12. González FG, Slafer GA, Miralles DJ. Pre-anthesis development and number of fertile florets in wheat as affected by photoperiod sensitivity genes Ppd-D1and Ppd-B1, Euphytica 146 (2005) 253–69. https://doi.org/10.1007/s10681-005-9021-3
13. Ramirez IA, Abbate PE, Redi IW, Pontaroli AC. Effects of photoperiod sensitivity genes *Ppd-B1* and *Ppd-D1* on spike fertility and related traits in bread wheat. Plant Breeding. 2018;137:320–5. https://doi.org/10.1111/pbr.12585.
14. Okada T, Jayasinghe JEARM, Eckermann P, Watson-Haigh NS, Warner P, Hendrikse Y, Baes M, Tucker EJ, Laga H, Kato K, Albertsen M, Wolters P, Fleury D, Baumann U, Whitford R. Effects of Rht-B1 and Ppd-D1 loci on pollinator traits in wheat. Theor Appl Genet. 2019;132:1965–79. https://doi.org/10.1007/s00122-019-03329-w.
15. Chen L, Yang Y, Cui C, Lu S, Lu Q, Du Y, Su R, Chai Y, Li H, Chen F, Yu F, Hu Y-G. Effects of Vrn-B1 and Ppd-D1 on developmental and agronomic traits in Rht5 dwarf plants of bread wheat. Field Crops Res. 2018;219:24–32. https://doi.org/10.1016/j.fcr.2018.01.022.
16. Zhang XK, Xiao YG, Zhang Y, Xia XC, Dubcovsky J, He ZH. Allelic Variation at the Vernalization Genes *Vrn-A1*, *Vrn-B1*, *Vrn-D1*, and *Vrn-B3* in Chinese Wheat Cultivars and Their Association with Growth Habit, Crop Science 48 (2008) 458–470. https://doi.org/10.2135/cropsci2007.06.0355
17. Smolenskaya SE, Goncharov NP. Allelic diversity of the *Vrn* genes and the control of growth habit and earliness in wheat. Vestn VOGiS. 2023;27:933–46. https://doi.org/10.18699/VJGB-23-108.
18. Mizuno N, Matsunaka H, Yanaka M, Nakata M, Nakamura K, Nakamaru A, Kiribuchi-Otobe C, Ishikawa G, Chono M, Hatta K, Fujita M, Kobayashi F. Allelic variations of *Vrn-1* and *Ppd-1* genes in Japanese wheat varieties reveal the genotype-environment interaction for heading time, Breed. Sci. 72 (2022) 343–354. https://doi.org/10.1270/jsbbs.22017
19. Plotnikov KO, Klimenko AI, Ovchinnikova ES, Lashin SA, Goncharov NP. Analysis of the Effects of the Vrn-1 and Ppd-1 Alleles on Adaptive and Agronomic Traits in Common Wheat (Triticum aestivum L. Plants. 2024;13:1453. https://doi.org/10.3390/plants13111453.
20. Iqbal M, Navabi A, Yang R, Salmon DF, Spaner D. The Effect of Vernalization Genes on Earliness and Related Agronomic Traits of Spring Wheat in Northern Growing Regions. Crop Sci. 2007;47:1031–9. https://doi.org/10.2135/cropsci2006.09.0618.
21. Kruijer W, Boer MP, Malosetti M, Flood PJ, Engel B, Kooke R, Keurentjes JJB, van Eeuwijk FA. Marker-Based Estimation of Heritability in Immortal Populations. Genetics. 2015;199:379–98. https://doi.org/10.1534/genetics.114.167916.
22. Yan W, Tinker NA. Biplot analysis of multi-environment trial data: Principles and applications. Can J Plant Sci. 2006;86:623–45. https://doi.org/10.4141/P05-169.

23. Bernatzky R, Tanksley SD. Genetics of actin-related sequences in tomato. Theoret Appl Genet. 1986;72:314–21. https://doi.org/10.1007/BF00288567.
24. Fu D, Szűcs P, Yan L, Helguera M, Skinner JS, von Zitzewitz J, Hayes PM, Dubcovsky J. Large deletions within the first intron in VRN-1 are associated with spring growth habit in barley and wheat. Mol Genet Genomics. 2005;273:54–65. https://doi.org/10.1007/s00438-004-1095-4.
25. Royston P. Remark AS R94: A Remark on Algorithm AS 181: The W-test for Normality. Appl Stat. 1995;44:547. https://doi.org/10.2307/2986146.
26. Jolliffe IT. Principal Component Analysis (2nd ed.), 2002.
27. Abdi H, Williams LJ. Principal component analysis. WIREs Comput Stats. 2010;2:433–59. https://doi.org/10.1002/wics.101.
28. Bates D, Mächler M, Bolker B, Walker S. Fitting Linear Mixed-Effects Models Using lme4. J Stat Softw. 2015;67:1–48. https://doi.org/10.18637/jss.v067.i01.
29. Brooks M, Kristensen EK, Benthem K, van Magnusson J, Berg C, Nielsen WA, Skaug H, Mächler JM, Bolker B. glmmTMB Balances Speed and Flexibility Among Packages for Zero-inflated Generalized Linear Mixed Modeling. R J. 2017;9:378. https://doi.org/10.32614/RJ-2017-066.
30. Kuznetsova A, Brockhoff PB, Christensen RHB. lmerTest Package: Tests in Linear Mixed Effects Models. J Stat Soft. 2017;82:1–26. https://doi.org/10.18637/jss.v082.i13.
31. Benjamini Y, Hochberg Y. Controlling the False Discovery Rate: A Practical and Powerful Approach to Multiple Testing. J Roy Stat Soc: Ser B (Methodol). 1995;57:289–300. https://doi.org/10.1111/j.2517-6161.1995.tb02031.x.
32. Pinheiro JC, Bates DM. Mixed-Effects Models in S and S-PLUS, 2000.
33. emmeans. Estimated marginal means, aka least-squares means. R package version 1.8.8, 2023.
34. Hothorn T, Bretz F, Westfall P. Simultaneous Inference in General Parametric Models. Biometrical J. 2008;50:346–63. https://doi.org/10.1002/bimj.200810425.
35. Nakagawa S, Schielzeth H. A general and simple method for obtaining R^2 from generalized linear mixed-effects models. Methods Ecol Evol. 2013;4:133–42. https://doi.org/10.1111/j.2041-210x.2012.00261.x.
36. Anderson MJ. A new method for non-parametric multivariate analysis of variance. Austral Ecol. 2001;26:32–46. https://doi.org/10.1111/j.1442-9993.2001.01070.pp.x.
37. vegan. Community Ecology Package. R package version 2.6-4, 2022.
38. Mahalanobis PC. On the generalised distance in statistics, Proceedings of the National Institute of Sciences of India 2 (1936) 49–55.
39. Hotelling H. The Generalization of Student's Ratio. Ann Math Statist. 1931;2:360–78. https://doi.org/10.1214/aoms/1177732979.
40. Venables WN, Ripley BD. Modern Applied Statistics with S (4th ed.), 2013.
41. Hollander M, Wolfe DA, Chicken E. Nonparametric Statistical Methods (3rd ed.), 2013.
42. R package. corrplot: Visualization of a Correlation Matrix (Version 0.92), 2021.
43. Divashuk MG, Bespalova LA, Vasilyev AV, Fesenko IA, Puzyrnaya OY, Karlov GI. Reduced height genes and their importance in winter wheat cultivars grown in southern Russia. Euphytica. 2013;190:137–44. https://doi.org/10.1007/s10681-012-0789-7.

44. DeWitt N, Guedira M, Lauer E, Murphy JP, Marshall D, Mergoum M, Johnson J, Holland JB, Brown-Guedira G. Characterizing the oligogenic architecture of plant growth phenotypes informs genomic selection approaches in a common wheat population. BMC Genomics. 2021;22:402–402. https://doi.org/10.1186/s12864-021-07574-6.
45. Amo A, Serikbay D, Song L, Chen L, Hu Y-G. Vernalization and photoperiod alleles greatly affected phenological and agronomic traits in bread wheat under autumn and spring sowing conditions. Crop Environ. 2022;1:241–50. https://doi.org/10.1016/j.crope.2022.11.002.
46. Makhoul M, Schlichtermann R-H, Ugwuanyi S, Weber SE, Voss-Fels KP, Stahl A, Zetzsche H, Wittkop B, Snowdon RJ, Obermeier C. Novel PHOTOPERIOD-1 gene variants associate with yield-related and root-angle traits in European bread wheat. Theor Appl Genet. 2024;137:125–125. https://doi.org/10.1007/s00122-024-04634-9.
47. Royo C, Dreisigacker S, Soriano JM, Lopes MS, Ammar K, Villegas D. Allelic Variation at the Vernalization Response (Vrn-1) and Photoperiod Sensitivity (Ppd-1) Genes and Their Association With the Development of Durum Wheat Landraces and Modern Cultivars, Front. Plant Sci. 2020;11. https://doi.org/10.3389/fpls.2020.00838.
48. Pourtabrizi S, Kazemipour A, Mohammadi-Nejad G, Khajoei-Nejad G, Abdolshahi R. Recessive Winter Growth Habit Allele on 5B Chromosome, vrn-B1, Improves Earliness and Grain Yield of Bread Wheat. J Plant Growth Regul. 2024;43:2830–40. https://doi.org/10.1007/s00344-024-11311-0.
49. Song T, Fan Q, Shi C, Li S, Zhou J, Bu Y, Chang X, Yu Y, Lei X, Wang Y, Chen D, Xiang J, Zhang X. Effects of five allelic variants of the wheat vernalization gene VRN-B1 on heading date and vernalization requirements. Mol Breed. 2025;45:44–44. https://doi.org/10.1007/s11032-025-01565-1.
50. Prieto P, Ochagavía H, Savin R, Griffiths S, Slafer GA. Dynamics of floret initiation/death determining spike fertility in wheat as affected by Ppd genes under field conditions. J Exp Bot. 2018;69:2633–45. https://doi.org/10.1093/jxb/ery105.
51. Ashfaq MQ, Qazalbash AA, Shaheen T, Javaid A, Waheed MQ, Arif A. Molecular evaluation of superior agronomic traits in local wheat germplasm using functional markers. Genet Resour Crop Evol. 2026;73. https://doi.org/10.1007/s10722-026-02760-5.

Figures

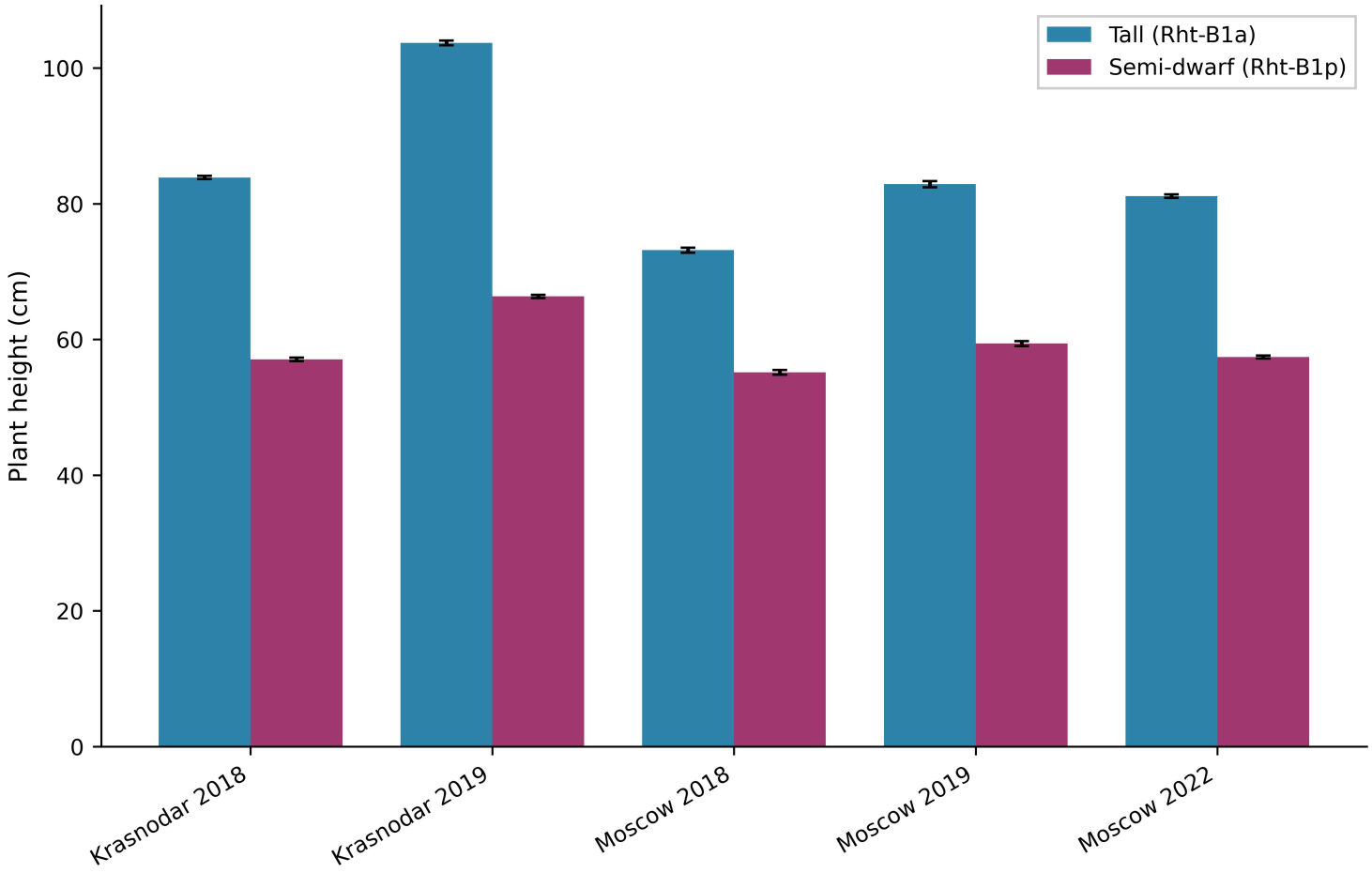


Figure 1

Plant height reduction by Rht-B1p across environments. Bars represent allele-class means in each location-year environment; error bars indicate +/-1 standard error.

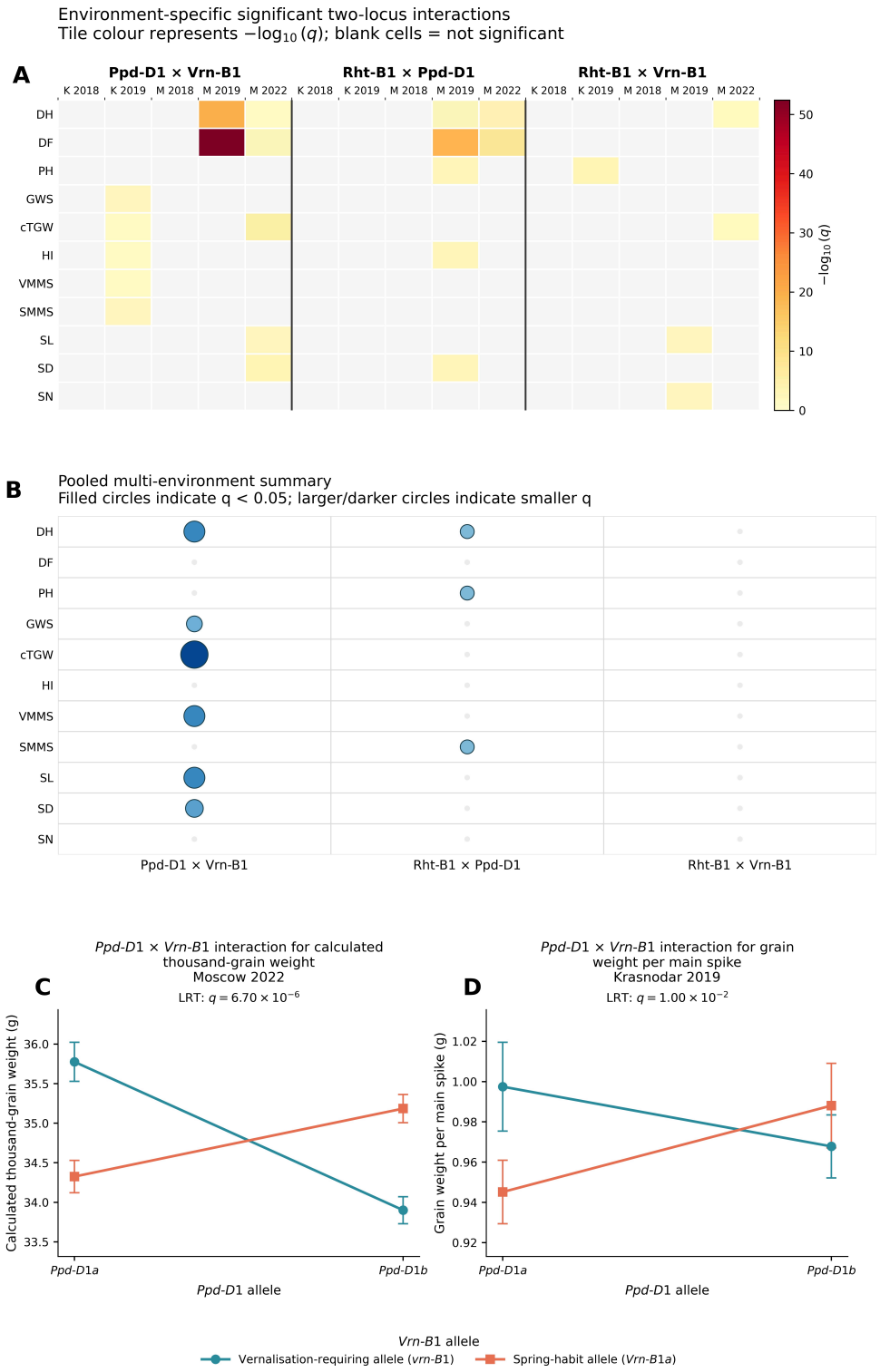


Figure 2

Two-locus interaction landscape across environments. (A) Heatmap of FDR-significant environment-specific interaction effects for the Ppd-D1 × Vrn-B1, Rht-B1 × Ppd-D1, and Rht-B1 × Vrn-B1 locus pairs across phenotypic traits and location–year environments. Cell colour represents −log10(q), with darker colours indicating stronger statistical evidence; blank cells indicate interactions that did not meet the FDR threshold of q < 0.05. K and M denote Krasnodar and Moscow, respectively. (B) Summary of FDR-significant interactions in the pooled multi-

environment analysis. Circle size and colour intensity are proportional to −log10(q); small pale circles indicate non-significant effects. (C) Interaction between Ppd-D1 and Vrn-B1 for calculated thousand-grain weight (cTGW) in Moscow 2022. (D) Interaction between Ppd-D1 and Vrn-B1 for grain weight per main spike (GWS) in Krasnodar 2019. In panels C and D, points represent raw allele-combination means and error bars indicate ±1 standard error. Teal circles denote the vernalisation-requiring vrn-B1 allele, and orange squares denote the spring-habit Vrn-B1a allele. Statistical significance of the interactions was evaluated using likelihood-ratio tests followed by Benjamini–Hochberg FDR correction.

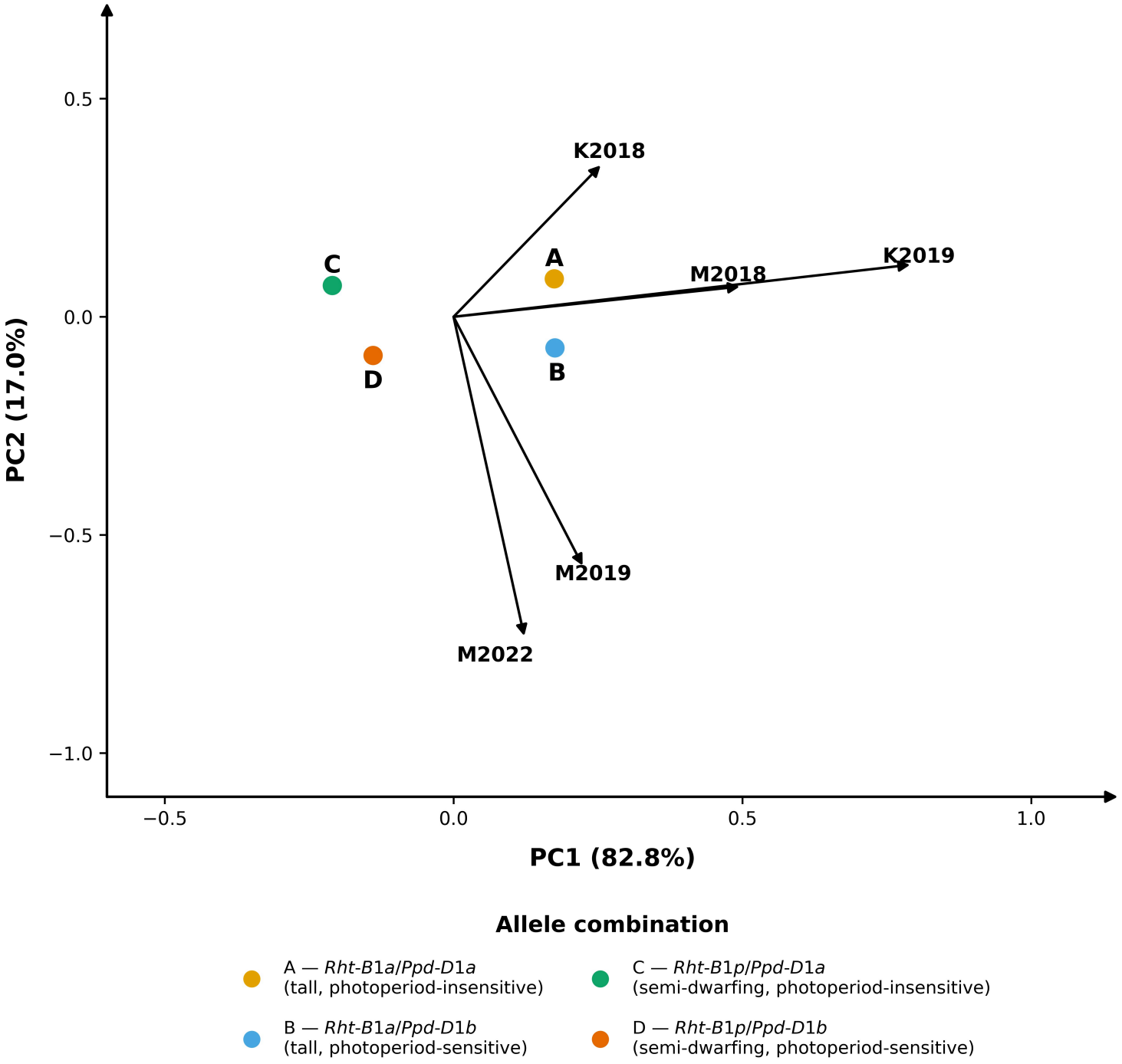


Figure 3

GGE biplot of Rht-B1 x Ppd-D1 combinations. PC1 and PC2 explained 82.8% and 17.0% of the environment-centred variation, respectively. Points represent allele combinations: (A) Rht-B1a/Ppd-D1a (tall, photoperiod-insensitive); (B) Rht-B1a/Ppd-D1b (tall, photoperiod-sensitive); (C) Rht-B1p/Ppd-D1a (semi-dwarfing, photoperiod-insensitive); and (D) Rht-B1p/Ppd-D1b (semi-dwarfing, photoperiod-sensitive). Arrows represent environment vectors: K2018 and K2019, Krasnodar 2018 and 2019; M2018, M2019, and M2022, Moscow 2018, 2019, and 2022. The projection of an allele combination onto an environment vector indicates its relative performance in that environment, with a larger positive projection corresponding to better adaptation or higher grain weight per main spike. In Moscow 2022, the tall, photoperiod-sensitive combination Rht-B1a/Ppd-D1b showed the highest projection and the highest mean grain weight per main spike (1.51 g), whereas the tall, photoperiod-insensitive combination Rht-B1a/Ppd-D1a showed a negative projection, indicating comparatively poor adaptation. The semi-dwarfing, photoperiod-sensitive combination Rht-B1p/Ppd-D1b combined reduced plant height with competitive productivity (1.49 g). Numerical projection values are provided in Supplementary Table S9.

Supplementary Files

This is a list of supplementary files associated with this preprint. Click to download.

- Additionalfile1Supplementaryinformation.docx
- Additionalfile2Perenvironmentstatisticalresults.xlsx
- Additionalfile3Pooledstatisticalresults.xlsx
- Additionalfile4Analysisdataset.xlsx
- Additionalfile5Analysiscode.zip